Smart Structures and Systems, *Vol. 33, No. 5 (2024) 359-364*
https://doi.org/10.12989/sss.2024.33.5.359

Computing of output of piezoelectric actuator under voltage excitation

Yongfeng Fang*[1], Kong Fah Tee [2,3a] and Yong Yan [1b]

[1] *Ningxia Normal University, School of Physics and Electric Information, Guyuan 756000, China*
[2] *Department of Civil and Environmental Engineering, King Fahd University of Petroleum and Minerals, Dhahran 31261, Saudi Arabia*
[3] *Interdisciplinary Research Center for Construction and Building Materials, KFUPM, Dhahran 31261, Saudi Arabia*

(*Received October 16, 2023, Revised March 29, 2024, Accepted April 1, 2024*)

Abstract. It is difficult to calculate the output force of a single-layer piezoelectric actuator under voltage excitation. In this paper, the piezoelectric actuator is organically combined with the mass-spring-damping system, and the deformation of the piezoelectric actuator under voltage excitation is transformed into the displacement of the mass-spring-damping system. Then, according to the differential equation of the system, the formulae of the mechanical output of the piezoelectric actuator under sinusoidal alternating current and DC step excitation are obtained by using the Laplace change and the inverse change, respectively. Finally, the proposed equations are verified by using ceramic piezoelectric actuators and PVDF actuators, respectively. The results are compared with the existing ones, which shows that the proposed method is feasible, easy, and practical.

Keywords: actuator; damping; output force; piezoelectric; voltage excitation

1. Introduction

As a new type of actuator, piezoelectric actuator (PA) is widely used in aerospace, medical and health, MEMS and other fields, and is playing an increasingly important role in smart manufacturing. The equation of the output voltage of a smart piezoelectric cantilever beam under vibration is established and the output voltage of the smart piezoelectric cantilever beam is analyzed. It is found that the output voltage of the smart piezoelectric cantilever beam has a positive proportional relationship by Fang *et al*. (2021). An offset piezoelectric pile actuator is studied. By integrating sensors and piezoelectric stack elements on the passive bearing structure, its damping performance to the elastic vibration of large space structure is evaluated by Francesca Callipari *et al*. (2022). The effect of nonlinear viscoelastic damping on the response of a cantilever sensor covered with symmetric or asymmetric piezoelectric layer is studied, and the effect of nonlinear piezoelectric damping on the application of scanning probe microscope sensors is discussed by Habib *et al*. (2022). The application of piezoelectric materials in the sensing field was studied and piezoelectric materials could sense the changes of micro and nano levels in mechanical sensing, and piezoelectric materials played an important role in the development of new sensing equipment by Qian *et al*. (2022).

The reliability of a piezoelectric actuator to alleviate the flutter of a flexible rectangular cantilever beam under wind load is investigated, the calculation model has practical engineering significance and feasibility for the reliability design and maintenance of unmanned aerial vehicle wings and wind power devices by Fang *et al*. (2023). The preparation of piezoelectric materials and their piezoelectric properties have been studied and it is believed that piezoelectric materials will provide a new path for the manufacture of wearable equipment and intelligent precision control equipment in the future by Wu *et al*. (2021). Among the piezoelectric materials, polyvinylidene fluoride and its copolymers have become the most promising piezoelectric nanogenerator materials due to their unique electrical activity, high flexibility, good machinability and long-term stability by Wang *et al*. (2021). A semi-passive nonlinear piezoelectric parallel absorber is proposed to reduce the vibration of resonant elastic structures under external excitation, and the design rules of free parameters of nonlinear systems are given by Shami *et al*. (2022).

Vibration is the main cause of structural cyclic failure, which can be reduced by piezoelectric components. The mechanical output performance of multilayer ceramic piezoelectric actuators was studied, and the critical voltage and maximum displacement of multilayer ceramic piezoelectric actuators were obtained by experimental method by Wang (2018), however, the results are not particularly accurate. To address the asymmetric and frequency-dependent hysteresis nonlinearity of ceramic piezoelectric actuators that cannot be described by most hysteresis models, an improved Bouc-Wen model was proposed and its compensation control was experimentally investigated based on the proposed improved Bouc-Wen model by ZHOU Minrui *et al*. (2023), but the mechanical output of piezoelectric actuator under different voltages is not given in this paper. The properties of a ceramic

*Corresponding author, Ph.D., Professor,
E-mail: fangyf_9707@126.com
[a] Ph.D., Professor
[b] Ph.D., Professor

ISSN: 1738-1584 (Print), 1738-1991 (Online)

piezoelectric stack actuator and its sensitivity were analyzed, and the results may be used for the analysis and design of piezoelectric actuators with different structural configurations. It is thought that the mechanical output of the piezoelectric actuator will greatly affect the sensitivity of the actuator by Jiang *et al*. (2023). The application of the piezoelectric flexibility actuator in gust load alleviation in the flexible wing was studied, and it is believed that piezoelectric actuators play an increasingly important role in gust load alleviation in the UAV wing by Versiani *et al*. (2019). Through the modeling and simulation of the active vibration control of the beam structure by piezoelectric actuator and sensor, it is considered that the piezoelectric actuator can effectively reduce the vibration amplitude of the beam by Robinson *et al*. (2021). The hysteresis characteristics and frequency correlation of the piezoelectric actuator with asymmetric characteristics were studied, and the displacement and velocity of the piezoelectric actuator were simulated. It was found that if the displacement control accuracy of the piezoelectric actuator was improved, then the robustness of the piezoelectric actuator could be effectively improved, and thus the positioning accuracy of the system would be significantly improved too by Xu *et al*. (2016). The roles and strategies of different smart materials in active vibration alleviation were described and it was specifically pointed out that piezoelectric stack actuator has good damping and frequency and good electromechanical coupling in active control, and it will play an important role in active vibration alleviation of the long-span structures in the future by Rasid *et al*. (2023). The vibration suppression performance of the piezoelectric actuator is studied, the structure is discretized by finite element method. The vibration modes are obtained by modal analysis and the maximum vibration amplitude is calculated by fast Fourier transform by Weimann *et al*. (2023). The piezoelectric impedance response sensitivity of damaged concrete in prestressed anchorage area is studied, the relationship between stress and output voltage under several overload conditions are analyzed by Dang *et al*. (2021). Piezoelectric actuators have been widely used in hard disk drives to form dual-stage actuation for position control. In the future, the piezoelectric micro-actuator will form triple-stage actuation, not only providing better position control accuracy, but also expanding micro-actuator design space by Liu (2023). A piezoelectric actuated micropump with integrated elastomeric was studied, the combination of this micropump with the 3D cell-culture microfluidic chip realizes the dynamic culture of cells encapsulated in 3D hydrogels with a continuous flowing medium by Holman *et al*. (2023). The electromechanical coupling of the piezoelectric bimorph beam was studied based on the simulation software Ansys. It was shown that the vibration suppression of the beam would become more significant with the increase of the circuit time constant and the electrical damping by Sun *et al*. (2017). The hysteresis characteristics and frequency correlation of the piezoelectric actuator with asymmetric characteristics were studied, and the displacement and velocity of the piezoelectric actuator were simulated. Many researches have shown that the piezoelectric actuator will play an important role in MEMS by Wang *et al*. (2022). However, so far, the mechanical output behaviour of the piezoelectric actuators has not been effectively investigated by using an electromechanical coupling system.

The electric power generation performance of a multilayer PVDF piezoelectric cantilever beam was studied, and the electric power generation effect of a cantilever beam with different layers and different arrangement of piezoelectric plates were obtained by simulation and experiment by Zhang *et al*. (2022). The application of the piezoelectric actuator in gust load alleviation in the flexible wing was studied, and it is believed that piezoelectric actuators play an increasingly important role in gust load alleviation in the UAV wing by Roy and Eversman (1996). So far, the mechanical output behaviour of piezoelectric actuators has not been effectively investigated by using an electromechanical coupling system.

It is not easy to accurately measure the mechanical output of a piezoelectric actuator. To be able to test the mechanical output of the piezoelectric actuator simply, quickly, and effectively, in this paper, based on the above literature, the piezoelectric actuator and the spring-mass-damping system will be organically combined, with the deformation of the piezoelectric actuator used to cause the movement of the spring-mass-damping system, and the Laplace transform and inverse transformation, the mechanical output computing model of the actuator under AC and DC excitation will be derived. Finally, the ceramic piezoelectric actuator and PVDF piezoelectric actuator can be calculated by using the proposed method, respectively, and the results will be compared with the results calculated by the existing methods in the literature.

2. Deformation of piezoelectric actuator

To calculate the mechanical output of the piezoelectric actuator, an electromechanical coupling system is designed as shown in Fig. 1. The left side of the system is the spring-mass-damping system (SMDS), and the right side is the external power supply and the piezoelectric actuator system.

In the electromechanical system, the three-dimensional constitutive equation of mechanical-electronic coupling of

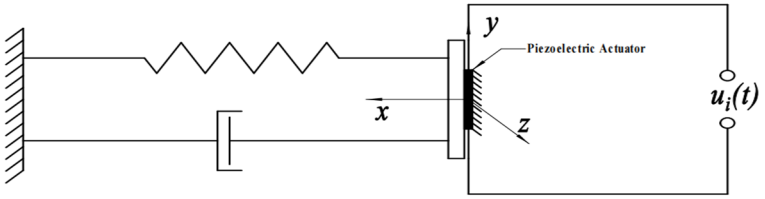

Fig. 1 The electromechanical coupling system

the piezoelectric material (PM) is shown as is shown as follows (Nanda and Nath 2012).

$$\boldsymbol{\varepsilon} = \boldsymbol{S\sigma} + \boldsymbol{e^T E} \tag{1}$$

$$\boldsymbol{D} = \boldsymbol{e\sigma} + \boldsymbol{KE} \tag{2}$$

where $\boldsymbol{\varepsilon}$ is the strain tensor of the PM, $\boldsymbol{\sigma}$ is the stress tensor of the PM, $\boldsymbol{D}$ is the electric displacement vector of the PM, $\boldsymbol{E}$ is the electric field intensity vector of the PM, **S**, **e**, **K** is the elastic compliance constant matrix, piezoelectric strain constant matrix and free dielectric constant matrix, respectively.

After polarizing the piezoelectric actuator along the *x* direction, then

$$\boldsymbol{e} = \begin{bmatrix} 0 & 0 & 0 & 0 & e_{15} & 0 \\ 0 & 0 & 0 & e_{24} & 0 & 0 \\ e_{31} & e_{32} & e_{33} & 0 & 0 & 0 \end{bmatrix}$$

$$\boldsymbol{K} = \begin{bmatrix} k_{11} & 0 & 0 \\ 0 & k_{22} & 0 \\ 0 & 0 & k_{33} \end{bmatrix}$$

$$\boldsymbol{S} = \begin{bmatrix} s_{11} & s_{12} & s_{13} & 0 & 0 & 0 \\ s_{21} & s_{22} & s_{23} & 0 & 0 & 0 \\ s_{31} & s_{32} & s_{33} & 0 & 0 & 0 \\ 0 & 0 & 0 & s_{44} & 0 & 0 \\ 0 & 0 & 0 & 0 & s_{55} & 0 \\ 0 & 0 & 0 & 0 & 0 & s_{66} \end{bmatrix}$$

x direction is the positive direction of the PA, then Eqs. (1) and (2) can be transformed into the one-dimensional form

$$\varepsilon_3 = s_{33}\sigma_3 + e_{33}E_3 \tag{3}$$

$$D_3 = e_{33}\sigma_3 + k_{33}E_3 \tag{4}$$

Eq. (5) can be derived by combining Eqs. (3) and (4) as follows

$$\varepsilon_3 = \frac{s_{33}}{e_{33}} \cdot D_3 + (e_{33} - \frac{s_{33}k_{33}}{e_{33}})E_3 \tag{5}$$

E_3 can be obtained as follows

$$E_3 = \frac{u_i(t)}{h} \tag{6}$$

where $u_i(t)$ is the externally applied voltage and h is the thickness of the piezoelectric plate.

Eq. (5) can be simplified as follows

$$\varepsilon_3 = \frac{s_{33}}{e_{33}} \cdot D_3 + \left(e_{33} - \frac{s_{33}k_{33}}{e_{33}}\right)\frac{u_i(t)}{h} \tag{7}$$

Eq. (7) is the output strain of the piezoelectric actuator under externally applied voltage.

The motion formula of the SMDS can be described as follows

$$\boldsymbol{M}\frac{d^2x(t)}{dt^2} + \boldsymbol{c}\frac{dx(t)}{dt} + \boldsymbol{K}x(t) = \boldsymbol{F}(t) \tag{8}$$

where **M** is the mass matrix, **c** is the damping matrix, **K** is the rigidity of the spring matrix, and **F(t)** is the external force.

x direction is the main direction, Eq. (8) can be simplified to one-dimensional form as follows

$$m\frac{d^2x(t)}{dt^2} + c\frac{dx(t)}{dt} + kx(t) = f(t) \tag{9}$$

3. Mechanical output of piezoelectric actuator

3.1 Mechanical output of PA under AC excitation

PA vibrates with the motion in *x* direction as follows

$$\varepsilon_3 \cdot h = x(t) = h \cdot \frac{s_{33}}{e_{33}} \cdot D_3 + \left(e_{33} - \frac{s_{33}k_{33}}{e_{33}}\right)u_i(t) \tag{10}$$

$$\frac{dx(t)}{dt} = \left(e_{33} - \frac{s_{33}k_{33}}{e_{33}}\right) \cdot \frac{du_i(t)}{dt} \tag{11}$$

$$\frac{d^2x(t)}{dt^2} = \left(e_{33} - \frac{s_{33}k_{33}}{e_{33}}\right) \cdot \frac{du_i{}^2(t)}{dt^2} \tag{12}$$

Eqs. (10)-(12) are substituted into Eq. (9)

$$f'(t) = A\left[m\frac{d^2u_i(t)}{dt^2} + c\frac{du_i(t)}{dt} + ku_i(t)\right] \tag{13}$$

where

$$f'^{(t)} = f(t) - k \cdot h \cdot \frac{s_{33}}{e_{33}}D_{33},$$

$$A = e_{33} - \frac{s_{33}k_{33}}{e_{33}}$$

The transfer function of Eq. (13) can be obtained by using the Laplace transform.

$$G(s) = \frac{F'(s)}{U_i(s)} = A(ms^2 + cs + k) \tag{14}$$

For PA, if AC is applied, the input signal can be assumed as follows

$$u_i(t) = A_1\, sin(\omega t + \phi) \tag{15}$$

where A_1 is the amplitude of the signal, ω is the frequency of the signal, and ϕ is the initial phase of the signal, its influence on the maximum mechanical output of the PA has not significant and can be ignored. Then, the Laplace transform of Eq. (15) is shown as follows

$$U_i(s) = A_1\frac{\omega}{s2 + \omega^2} \tag{16}$$

The mechanical output of the PA under the AC excitation is shown as follows

$$\begin{aligned} f'(t) = A \cdot A_1\big[&m(\omega \cdot dirac(t) - \omega^2\, sin(\omega t)\big) \\ &+\omega \cdot c \cdot cos(\omega t) + k\, sin(\omega t)] \end{aligned} \tag{17}$$

Eq. (17) can be further simplified, and the final mechanical output of the PA under AC input can be rewritten as follows

$$f(t) = \left(e_{33} - \frac{s_{33}k_{33}}{e_{33}}\right) \cdot A_1[m(\omega \cdot dirac(t) - \omega^2 sin(\omega t)) + \omega \cdot c \cdot cos(\omega t) + k\, sin(\omega t)] + h \cdot k \cdot \frac{s_{33}}{e_{33}} D_{33} \quad (18)$$

3.2 Mechanical output of PA under DC excitation

DC is applied on the PA, the input signal can be assumed as a step signal

$$u_i(t) = A_2 \quad (19)$$

Eq. (19) can be transformed by using Laplace transform as follows

$$U_i(s) = A_2 \cdot \frac{1}{s} \quad (20)$$

The mechanical output of the PA under the DC excitation is shown as follows

$$f^{'}(t) = A \cdot A_2(m \cdot dirac(t,1) + c \cdot \delta(t) + k) \quad (21)$$

Eq. (21) can be further simplified, and the final mechanical output of the PA under DC input can be rewritten as follows

$$f(t) = \left(e_{33} - \frac{s_{33}k_{33}}{e_{33}}\right) \cdot A_2(m \cdot dirac(t,1) + c \cdot \delta(t) + k) + h \cdot k \cdot \frac{s_{33}}{e_{33}} D_{33} \quad (22)$$

3.3 Computation of D3

As the electric displacement value after the piezoelectric material is polarized along the x-axis, D_3 plays an important role in the mechanical output of the piezoelectric actuator. Meanwhile, it increases the difficulty in the calculation of the mechanical output of the PA, so it is necessary to further simplify the processing of D_3.

The electric displacement vector is determined by the amount of surface charge of the PA and the effective area of the PA, which is given by the following equation

$$D_3 = \frac{q}{A} \quad (23)$$

where A is the effective area of the PA, q is the amount of surface charge of the PA and can be obtained as follows.

$$q = e_{33} f + C u_t(t) \quad (24)$$

C is equivalent capacitance, and f is the prestress applied to piezoelectric plates.

$$C = k_{33} \frac{wl}{h} \quad (25)$$

$$f = \frac{a_p}{a+1} l_s \quad (26)$$

where w is the width of the PA, l is the length of the PA, l_s is the amount of spring pre-deformation in the SMDS, a_p is the equivalent stiffness of the piezoelectric plate, a is the stiffness ratio of the piezoelectric material to the spring. According to the method in literature (Sun *et al.* 2017), a can be obtained by reasoning calculation and it generally takes the value of 4-15.

$$a_p = \frac{E_p w h^3}{4l^3} \quad (27)$$

4. Case study

To verify the effectiveness, accuracy and feasibility of the proposed method, two case studies are used as described below:

Case Study 1:

In reference (Wang 2018), the data obtained from multiple experiments and regression analysis are used. a_p is 6.72×10^4 N/m which can be obtained by using Eq. (27), f is 22.75 N which can be obtained by using Eq. (26), C is 84.6 F which can be obtained by using Eq. (25). According to the method in the reference, the mechanical output of

Table 1 The parameters of the ceramic actuator

Parameter	Value
s_{33}	15.6×10^{-12} m^2/N
e_{33}	315×10^{-12} C/N
h	1×10^{-3}m
c	100 N·s/m
w	12 mm
l_s	1.693 mm
k_{33}	470 F/m
E_p	7.56×10^{10} N/m^2
k	3931.7 N/mm
m	10 kg
l	15 mm

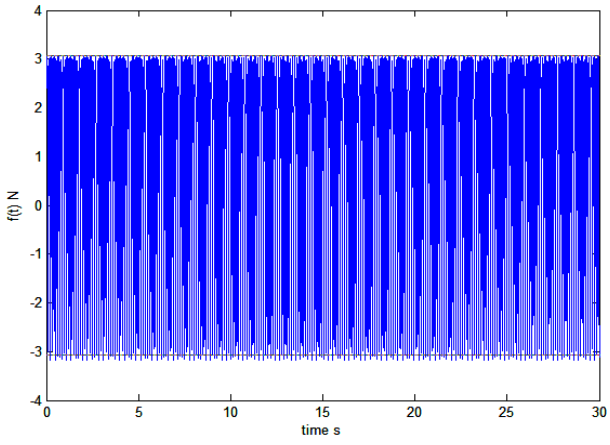

Fig. 2 The mechanical output of the piezoelectric ceramic actuator under the AC excitation

a single ceramic piezoelectric actuator is 3.08 N under the excitation of 500 V voltage. The relevant parameters of piezoelectric ceramics provided by the literature are shown in Table 1.

Based on Eq. (22), a mechanical output calculated is 3.08 N with an excitation voltage of 500 V DC. On the other hand, a mechanical output calculated with the input voltage of 500 V and the frequency of 50 AC excitation voltage calculated once with Eq. (18) is shown in Fig. 2.

It is shown in Fig. 2, even if the excitation power is AC with a voltage amplitude of 500 and a frequency of 5, the mechanical output of the PA is between [-3.08 N, 3.08 N] in 30 seconds. The results are highly consistent with the literature (Wang 2018) which was obtained by using the experimental regression method. It is indicated that the proposed method is feasible and effective in calculating the mechanical output of ceramic piezoelectric actuators.

Case Study 2:

In reference (Sun *et al*. 2017), 4 layer PVDF is investigated, and the relationship between voltage and actuator power is given. a_p is 0.1365 N/m which can be obtained by using Eq. (27), f is 5.733×10^4 N which can be obtained by using Eq. (26), C is 3.2×10^{-8} F which can be obtained by using Eq. (25). According to the parameters and methods provided in this reference, the mechanical output of a single-layer PVDF actuator is 0.6832 N under the excitation of 34 V voltage. The parameters of PVDF provided in this reference are shown in Table 2.

Table 2 The parameters of PVDF

Parameter	Value
s_{33}	3.33×10^{-10} M^2/N
e_{33}	28.1×10^{-12} C/N
h	0.11×10^{-3} m
c	100 N·s/m
w	8 mm
l_s	21 mm
k_{33}	110×10^{-12} F/m
E_p	3×10^9 N/m^2
k	666 N/mm
m	0.07512 kg
l	40 mm

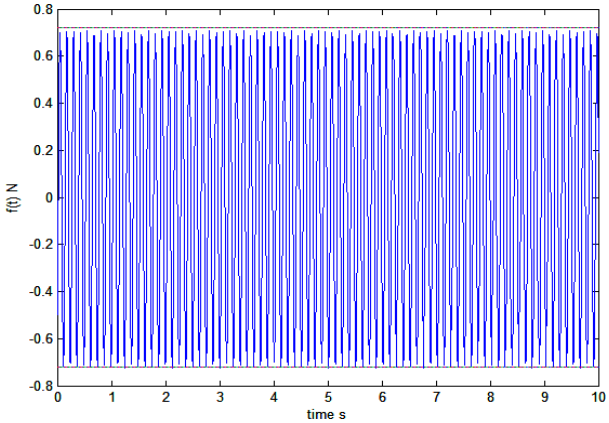

Fig. 3 The mechanical output of the PVDF actuator under the AC excitation

Based on Eq. (22), the excitation voltage is 34 V DC, and its mechanical output is 0.6832 N. On the other hand, according to Eq. (18), the input voltage is 34 V AC and the frequency is 50, the mechanical output in 10 seconds is shown in Fig. 3.

It is shown that even if the excitation voltage amplitude is 34V and the AC frequency is 50, its mechanical output in 10 seconds is between [-0.6832, 0.6832] N. The results are highly consistent with the result in the literature (Sun *et al*. 2017) which was obtained by electron microscope scanning. It is indicated that the proposed method is feasible, simple and effective in calculating the mechanical output of PVDF piezoelectric actuators.

5. Conclusions

In this paper, for the problem that the mechanical output of a single-layer piezoelectric actuator is difficult to compute. The piezoelectric actuator and spring-mass-damping system are organically combined. The motion of the spring-mass-damping system is caused by the deformation of the piezoelectric actuator, and the differential equation of motion is established. Then, the derivation of the mechanical output of the actuator under AC and DC excitation is established by using the Laplace transform method and inverse transformation method. Finally, the ceramic piezoelectric actuator and PVDF piezoelectric actuator are calculated by using the method, respectively. The calculated results are compared with those in the reference, it is shown that the proposed method is effective, feasible and practical.

Acknowledgments

The work described in this paper was supported in part by the Ningxia key research and development program, China (2020BEB4040, 2022BSB03101), Ningxia fundamental research project (2022AAC3335, 2023AAC03332, 2023AAC03339, 2023AAC 03353), NSFC (12365025) and the university research project of Ningxia (NYG2024167).

References

Callipari, F., Sabatini, M., Angeletti, F., Iannelli, P. and Gasbarri, P. (2022), "Active vibration control of large space structures: Modelling and experimental testing of offset piezoelectric stack actuators", *Acta Astronautica*, **198**, 733-745. https://doi.org/10.1016/j.actaastro.2022.05.058

Dang, N.L., Pham, Q.Q. and Kim, J.T. (2021), "Piezoelectric skin sensor for electromechanical impedance responses sensitive to concrete damage in prestressed anchorage zone", *Smart Struct. Syst., Int. J.*, **28**(6), 761-777. https://doi.org/10.12989/sss.2021.28.6.761

Fang Y, Tee, K.F. and Wen, L. (2021), "Analytical solution of monomorph and bimorph piezoelectric cantilever beams",

Sensors Mater., **33**(7), 2407-2413. https://doi.org/10.18494/SAM.2021.3210

Fang, Y., Fang, Z., Tee, K.F. and Tuo, Y. (2023), "Reliability computation of piezoelectric actuator embedded in flexible smart rectangle cantilever beam under complex gust load", *Sensors Mater*., **35**(5), 1741-1751. https://doi.org/10.18494/SAM4345

Habib, G., Fainshtein, E., Wolf, K.D. and Gottlieb, O. (2022), "The influence of nonlinear damping on the response of a piezoelectric cantilever sensor in a symmetric or asymmetric configuration", *Smart Struct. Syst*., *Int. J*., **30**(3), 239-243. https://doi.org.10.12989/sss.2022.30.3.239

Holman, J.B., Zhu, X. and Cheng, H. (2023), "Piezoelectric micropump with integrated elastomeric check valves: design, performance characterization and primary application for 3D cell culture", *Biomed. Microdev*., **25**, 5-20. https://doi.org/10.1007/s10544-022-00645-9

Jiang, X., Zheng, J., Wang, N. and Pan, J. (2023), "Sensitivity of piezoelectric stack actuators", *Sensors*, **23**, 9542. https://doi.org/10.3390/s23239542

Liu, Y. (2023), "Advance piezo-actuator technologies for hard disk drive applications", *Microsyst. Technol*., **29**, 1117-1127. https://doi.org/10.1007/s00542-023-05460-7

Nanda, N. and Nath, Y. (2012), "Active control of delaminated composite shells with piezoelectric sensor/actuator patches", *Struct. Eng. Mech*., *Int. J*., **42**(2), 211-228. https://doi.org.10.12989/sem.2012.42.2.211

Qian, L., Li, Y., Sun, Q. and Ge, J.Y. (2022), "Dynamic characteristics study of PVDF shock sensor", *Transd. Microsyst. Technol*., **41**(7), 33-37. https://doi.org.10.13873/J.1000-9787(2022)07-0033-04

Rasid, S.M.R., Michael, A. and Pota, H.R. (2023), "Dynamic modeling of a piezoelectric micro-lens actuator with experimental validation", *Sensors Actuators A*: *Phys*., **356**(16), 114344. https://doi.org/10.1016/j.sna.2023.114344

Robinson, P., Vishwanath, K.H. and Ashwini, M.V. (2021), "A study on structural analysis of composite beam structure", *Materials Today*: *Proceedings*, **45**, 434-439. https://doi.org/10.1016/J.MATPR.2020.12.1154

Roy, I.D. and Eversman, W. (1996), "Adaptive flutter suppression of an unswept wing", *J. Aircraft*, **33**(4), 775-783. https://doi.org/10.2514/3.47014

Shami, Z.A., Giraud-Audine, C. and Thomas, O. (2022), "A nonlinear piezoelectric shunt absorber with a 2:1 internal resonance: Theory", *Mech. Syst. Signal Process*., **170**, 108768. https://doi.org/10.1016/j.ymssp.2021.108768

Sun, K., Wang, H.F., Li, M. and Cui, Y.L. (2017), "Analysis of electrical damping of piezoelectric bimorph actuator", *J. Qingdao Univ*. (*Natural Science Ed*.), **30**(4), 84-88. https://doi.org.10.3969/j.issn.1006-1037.2014.11.16

Versiani, T.D.S.S., Silvestre, F.J., Neto, A.B.G., Rade, D.A., da Silva, R.G.A., Donadon, M.V., Bertolin, R.M. and Silva, G.C. (2019), "Gust load alleviation in a flexible smart idealized wing", *Aerosp. Sci. Technol*., **86**, 762-774. https://doi.org/10.1016/jast.2019.01.058

Wang, B. (2018), "System reliability analysis of piezoelectric truss structures", Ph.D. Dissertation; Harbin Engineering University, Harbin, China.

Wang, Y., Zhu, L. and Du, C. (2021), "Progress in piezoelectric nanogenerators based on PVDF composite films", *Micromach*., **12**, 1278. https://doi.org/10.3390/mi12111278

Wang, H., Li, Y., Hui, H. and Rong, T. (2022), "Analysis of electromechanical characteristics of the 1-3-2 piezoelectric composite and 1-3-2 modified structural material", *Ceramics Int*., **48**, 22323-22334. https://doi.org.10.1016/j.ceramint.2022.04.238

Weimann, T., Molter, A., Fernandez, L. and He, M. (2023), "Structural vibration control based on the effect of acoustic black holes and piezoelectric actuators", *Finite Elem. Anal. Des*., **224**(15), 103992. https://doi.org/10.1016/j.finel.2023.103992

Wu, Y., Ma, Y., Zheng, H. and Ramakrishna, S. (2021), "Piezoelectric materials for flexible and wearable electronics: A review", *Mater. Des*., **211**, 110164. https://doi.org/10.1016/j.matdes.2021.110164

Xu, L., Li, H. and Li, C. (2016), "Displacements of the flexible ring for an electromechanical integrated harmonic piezodrive system", *Struct. Eng. Mech*., *Int. J*., **60**(6), 1079-1092. https://doi.org.10.12989/sem.2016.60.6.1079

Zhang, X., Chen, L. Wang, L. and She, X. (2022), "Power output characteristics analysis of multilayer PVDF stacked piezoelectric cantilever beam", *J. Vib. Shock*, **41**(5), 217-224. https://doi.org.10.13465./j.cnki.jvs.2022.15.028

Zhou, M.R., Zhou, Z.H., Liu, X., Cao, T.S. and Li, Z.H. (2023), "Improved Bouc-Wen model of piezoelectric actuator and its positioning compensation control study", *J. Vib. Shock*, **42**(10), 155-164. https://doi.org.10.13465/j.cnki.jvs.2023.10.019